# Crystal Nucleation without Supersaturation

**ARTICLE** *in* JOURNAL OF PHYSICAL CHEMISTRY LETTERS · JUNE 2012

Impact Factor: 7.46 · DOI: 10.1021/jz300450g



**3 AUTHORS:**

Tamás Kovács
University of Leeds
**26** PUBLICATIONS **176** CITATIONS
SEE PROFILE

Fiona C. Meldrum
University of Leeds
**130** PUBLICATIONS **6,772** CITATIONS
SEE PROFILE

Hugo K Christenson
University of Leeds
**126** PUBLICATIONS **5,498** CITATIONS
SEE PROFILE

THE JOURNAL OF PHYSICAL CHEMISTRY Letters

Letter

pubs.acs.org/JPCL

# Crystal Nucleation without Supersaturation

T. Kovács,[†] F. C. Meldrum,[‡] and H. K. Christenson*,[†]

[†]School of Physics and Astronomy and [‡]School of Chemistry, University of Leeds, Leeds LS2 9JT, United Kingdom

Supporting Information

**ABSTRACT:** Classical nucleation theory (CNT) has been extensively employed to interpret crystal nucleation phenomena and postulates the formation of an ordered crystalline nucleus directly from vapor or solution. Here, we provide the first experimental demonstration of a two-step mechanism that facilitates deposition of crystals on solid surfaces from vapor. Crucially, this occurs from saturated vapor without the need for supersaturation, conditions that, according to CNT, cannot lead to direct deposition of crystals from vapor. Instead, the process relies on condensation of supercooled liquid in surface cavities below the melting point. Crystals then nucleate in this liquid, leading to rapid deposition of more solid. Such a mechanism has been postulated for atmospheric nucleation of ice on aerosol particles and may have analogies in the crystallization of biominerals via amorphous precursor phases.

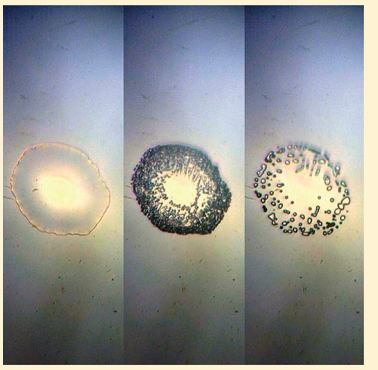

**SECTION:** Surfaces, Interfaces, Porous Materials, and Catalysis

Classical nucleation theory (CNT) describes nucleation processes and how they depend on factors like supersaturation, absolute concentrations, and, for heterogeneous nucleation, interactions with the surface. It predicts a free-energy barrier to nucleation due to the cost of creating an interface between the old and the incipient phase. Despite often large quantitative discrepancies between the predictions and experimental measurements, CNT is useful as a starting point for the consideration of nucleation. However, it is becoming increasingly clear that many nucleation processes do not conform to the classical model, which relies on a sufficient number of molecules coming together to form a nucleus that immediately adopts the structure of the new phase. In its place, experiments and computer simulations have shown that crystal nucleation may be mediated by denser fluid precursor phases[1−7] or clusters of molecules[8,9] from which the final crystal forms. It has been shown both experimentally and theoretically that such two-step mechanisms may lead to a significant enhancement of nucleation rates of proteins and colloids as well as smaller molecules.[5,7,8]

Crystallization of solid from vapor is typically associated with a much larger free-energy barrier than crystallization from solution or from the melt as the free energy of a solid surface in vapor is unusually high. The nucleation of crystals from vapor is therefore particularly unfavorable, even on surfaces, and ice nucleation on solid aerosols in cirrus clouds,[10] for example, requires supersaturation of the vapor phase by 20−50%. However, according to CNT, substrate geometries such as surface cavities, which increase the substrate−nucleus area at the expense of the vapor−substrate area, are expected to facilitate nucleation.[11,12]

As liquids usually have lower surface energies than solids, crystals often deposit on a substrate from vapor via an undercooled liquid. Surface cavities can also facilitate liquid condensation as there is rarely an energy barrier toward condensation in an acute wedge, and it occurs even from undersaturated vapor. This process is termed capillary condensation, and it also occurs below the bulk melting temperature $T_m$ as the smaller interfacial free energy between the substrate and a liquid than that between the substrate and a crystal favors the liquid state.[13,14] Whereas a liquid condensate grows indefinitely at saturation above $T_m$, below $T_m$, its size is limited as there cannot be equilibrium between saturated vapor and bulk liquid below $T_m$. The total radius of curvature $r$ of the liquid−vapor interface in saturated vapor is inversely proportional to the temperature depression $\Delta T$ below $T_m$ ($\Delta T = T_m - T$, the actual temperature), and for small $\Delta T$, iy is given by[14]

$$\frac{1}{r} = \frac{\Delta H_{fus} \Delta T}{V_{ML} \gamma_{LV} T_m} \quad (1)$$

where $\gamma_{LV}$ is the surface energy of the liquid, $V_{ML}$ its molar volume, and $\Delta H_{fus}$ its enthalpy of fusion (inclusion of the temperature dependence of the surface tension and the enthalpy of melting means that $1/r$ versus $\Delta T$ becomes nonlinear for large $\Delta T$).[14]

Consequently, in a conical or wedge-shaped pore, a condensate only grows until its liquid−vapor interface satisfies eq 1. However, a simple analysis shows that a region of the condensates next to the liquid−vapor interface is metastable toward freezing, provided the surface tension $\gamma_{LV}$ is more than twice as large as $\gamma_{SL}$, the interfacial tension between the liquid and its solid, which is true for most common substances (see

**Received:** April 14, 2012
**Accepted:** May 30, 2012

   dx.doi.org/10.1021/jz300450g | J. Phys. Chem. Lett. XXXX, XXX, XXX−XXX

Supporting Information).[14] If this region were to crystallize or freeze, it could provide an alternative route to the deposition of solid from vapor. Capillary condensation below $T_m$ does not require supersaturation of the vapor phase, and crystals may then nucleate in the liquid condensates if the undercooling below $T_m$ is large enough. Once crystals have nucleated and if the vapor is saturated, these crystals can grow indefinitely as the saturated vapor is in equilibrium with bulk solid below $T_m$.

In this Letter, we investigate the viability of this mechanism as a means of achieving greatly enhanced deposition of solid from vapor that is maintained exactly at saturation. Three contrasting model substances having $T_m$ above room temperature and reasonably high saturation vapor pressures $p_{sat}$ at room temperature were selected for study: hexamethylcyclotrisiloxane (HMCTS), $p_{sat}$ (25 °C) = 5 mm of Hg,[15] $T_m$ = 64.5 °C; [16] *neo*-pentanol, $p_{sat}$ (25 °C) = 16 mm of Hg,[17] $T_m$ = 52.5 °C;[16] and norbornane, $p_{sat}$ (25 °C) = 28 mm of Hg,[18] $T_m$ = 87.5 °C[16]). More information on the physical properties is given in the Supporting Information.

The investigation was carried out using a simplified[19,20] surface force apparatus that has previously been used in a range of capillary condensation experiments.[19−24] In the experiments, two curved (radius of curvature $R$ = 2 cm) mica surfaces in a crossed cylinder configuration are brought into contact in saturated vapor below $T_m$ in a sealed, temperature-controlled chamber. The presence and effect of capillary condensates is deduced from the appearance and wavelength shifts of optical interference fringes (see the Experimental Methods section). The surfaces are pulled into contact (separated by a few molecular layers) from separations of 10−20 nm by the negative Laplace pressure in a liquid capillary condensate,[20] which forms by a film-thickening mechanism.[21] These jump distances are typical of substances below $T_m$ where only about two molecular layers are adsorbed on isolated surfaces[14,22] (the film thickness $t$ in Figure 1). In agreement with this, the liquid

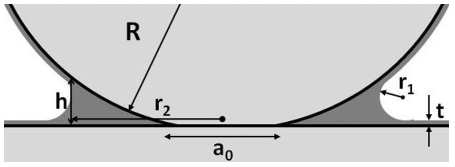


**Figure 1.** Schematic cross section of crossed mica cylinders in the equivalent sphere-on-a-flat configuration, with a liquid capillary condensate around the flattened contact region. Typically, $R$ = 2 cm, $a_0 \approx 25$ μm, $r_2 \approx +13-50$ μm, and $h \approx (5$ nm−1 μm). For liquids, $h$ is related to the radius of curvature of the vapor−condensate interface $r_1$ and the thickness $t$ (typically ∼1 nm) of the adsorbed film on the surfaces by $h = 2|r_1| + 3t$. For large, solid condensates $h = 2r_1$ is correct within error. Because $|r_1| \ll |r_2|$, the total radius of curvature of the interface is $r \approx r_1$.

phase of the substances studied here show typically small but nonzero contact angles on the mica surfaces. Thicker films above $T_m$ may give rise to much larger jumps.[21] As they come into contact, the mica surfaces flatten (Figure 1) due to their large $R$ and the relatively soft glue used to mount them.[25] The flattened mica surfaces in contact form an annular wedge in which liquid will condense from the saturated vapor until the separation $h$ between the mica surfaces at the liquid−vapor interface is very nearly equal to twice the interfacial radius of curvature given by eq 1 (see the Experimental Methods section and Figure 1).

In what follows, undercooling (the value of $\Delta T$) always refers to the temperature depression below the bulk solid−liquid (melting) transition. Capillary condensation of all three substances from saturated vapor was studied as a function of $\Delta T$, and three regimes of behavior were identified. For undercoolings below $T_m$ of $\Delta T \leq 18$ K (*neo*-pentanol) or $\Delta T \leq 33$ K (HMCTS), a liquid condensate of limited size described initially forms around the contact zone (Figure 2a−c). That the condensate is liquid is demonstrated by separating the surfaces, in which case the diameters of both the flattened contact area and the liquid condensate decrease smoothly until the surfaces come apart and the annulus turns into a bridging

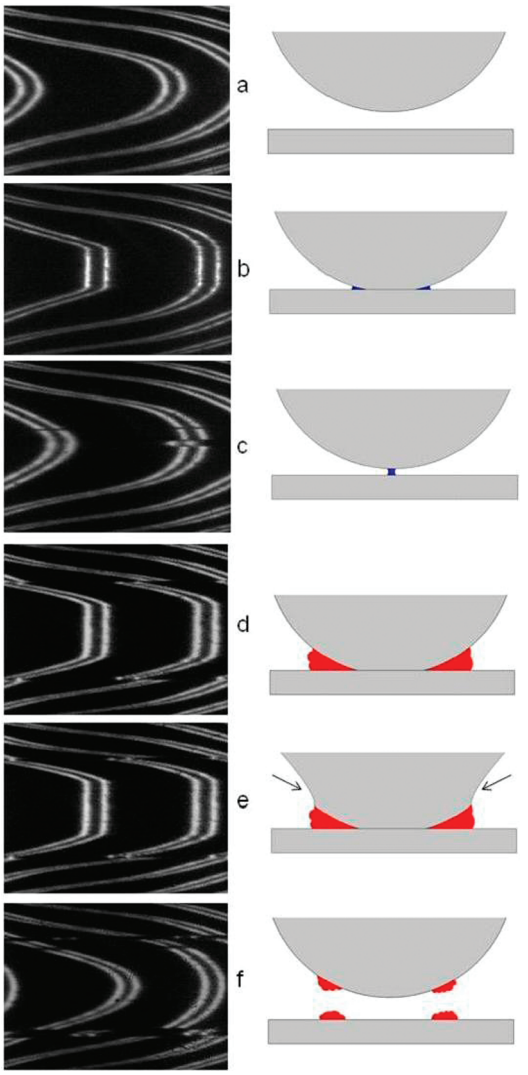


**Figure 2.** Interference fringes and the surface configuration deduced therefrom for mica surfaces in *neo*-pentanol vapor. The wavelength increases toward the left. The fringes are doublets due to the birefringence of mica, and their shape reflects the increasing surface separation on going away from the point of closest approach at the center and the surface flattening when the surfaces are in contact. Discontinuities can be seen where the refractive index changes abruptly for that of the vapor to the condensed phase. Surfaces (a) ∼50 nm apart in vapor, (b) in contact in *neo*-pentanol vapor, (and c) after separation from contact with liquid bridge (a−c all at $\Delta T$ = 28 K). Surfaces (d) in contact with solid annulus of $h \approx 200$ nm, (e) that deform as they are pulled apart (arrows), and (f) after a large jump apart, showing solid residue on surfaces (d−f all at $\Delta T$ = 33 K).


dx.doi.org/10.1021/jz300450g | J. Phys. Chem. Lett. XXXX, XXX, XXX−XXX

neck, which quickly evaporates (Figure 2c). No liquid condensates can be observed with norbornane as the minimum undercooling below $T_m$ achievable with our system is 37 K.

At the largest undercoolings below $T_m$ ($\Delta T$ > 34 K), the behavior is very different, and with all three substances, a condensate grows rapidly immediately after the surfaces come into contact (Figure 3d). Condensate sizes, $h$ (as defined in

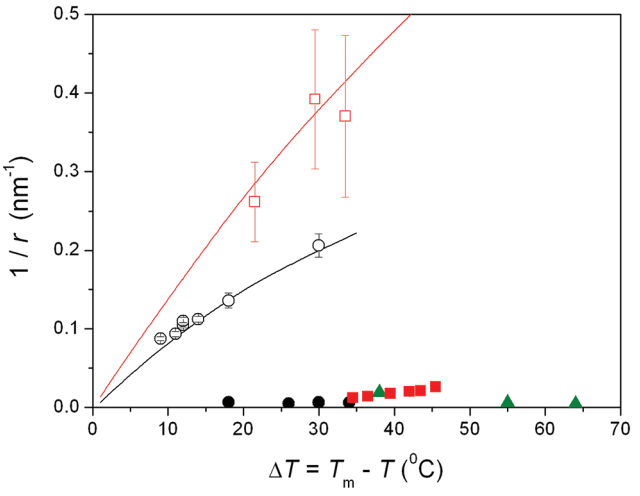


**Figure 3.** The inverse of the radius of curvature $r$ (=$(h - 3t)/2$) of the condensate–vapor interface for condensates of liquid *neo*-pentanol (open circles), liquid HMCTS (open squares), solid *neo*-pentanol (filled circles), solid HMCTS (filled squares), and solid norbornane (filled triangles) as a function of the temperature depression $\Delta T$ below the bulk melting point (i.e., temperature decreases toward the right). The temperature dependence of the surface tension and the enthalpy of fusion cause the $1/r$ versus $\Delta T$ dependence to deviate from linearity (eq 1) as $\Delta T$ increases[14] (solid lines). Note the very significant increase in condensate size (decrease in $1/r$) for solid condensates (where $h = 2r$ with negligible error.

Figure 1) of between 200 nm (HMCTS) and 2 $\mu$m (norbornane) were observed within 30 min. The contact diameter of the surfaces cannot be changed by loading or unloading, but instead, the surfaces deform beyond the condensate (Figure 2e). The force required to separate the surfaces is about an order of magnitude larger than that with the liquid condensate. This shows that the condensate is solid and "glues" the surfaces together. Upon separation, an annular deposit of material is left on both surfaces (Figure 2f), and this evaporates over minutes because small, convex crystallites are unstable even in saturated vapor due to the enhanced vapor pressure over a convex surface.

At intermediate temperatures below $T_m$ (18 < $\Delta T$ < 30 for *neo*-pentanol and at $\Delta T \approx 34$ K for HMCTS), the initial condensate is liquid, but rapid deposition of crystalline material is frequently initiated, likely in response to an external stimulus (e.g., vibration). Alternatively, rapid deposition can be induced by increasing the load slightly, which perturbs the surfaces, and then unloading the surfaces. This rapidly depositing material is clearly solid, as explained above, although the innermost region of the condensate almost certainly remains liquid, as expected on theoretical grounds.[14,26]

The substantial difference in size between the solid deposits (filled symbols) and liquid condensates (open symbols) is shown in Figure 3. The quantity measured from the fringes is condensate size (Figure 1), and this is related to the total radius of curvature $r$ of a liquid condensate by $h = 2r + 3t$,[27] where $t$ is the thickness of films adsorbed on an isolated mica surface at the same temperature (of the order of 1 nm below $T_m$). We have plotted the size as $1/r$ versus $\Delta T$ as this shows that behavior of the liquid condensates is well described by theory[14] (solid lines). We do not know whether interfacial curvature has any significance for the solid deposits, but as $t$ is negligible compared to $r$, for the large solid deposits, we can set $h = 2r$. The error bars for HMCTS are large as the condensate is too small for its size to be directly measured with the surfaces in contact, and it can only be estimated from the size of the liquid neck immediately after separation of the surfaces. With norbornane, only very large solid condensates are observed at undercoolings below $T_m$ of $\Delta T$ > 37 K.

The solid condensates are also visible in a microscope by observing the mica surfaces from above (Figure 4), which

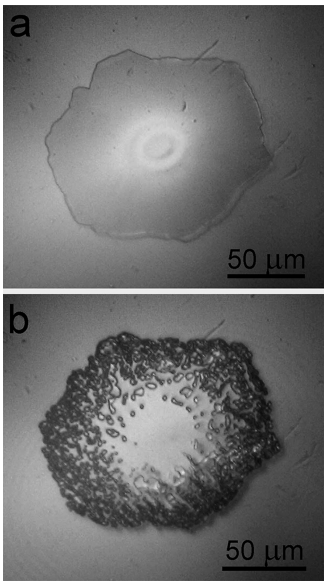


**Figure 4.** Microscope image taken from above a solid norbornane deposit in the annular wedge between crossed mica cylinders (a) after nucleation in a liquid capillary condensate formed in saturated vapor at 52 K below the melting point. The bright center region is mica–mica contact, and the norbornane vapor interface is an irregular hexagon. Upon separation, the crystalline condensate joining the surfaces shatters (b).

enables the process of separation to be followed. As the surfaces come apart, the solid norbornane condensate shatters into fragments tht then evaporate, as expected for highly convex particles in a saturated atmosphere. Finally, that this route to nucleation is not surface-specific is shown by the formation of analogous solid deposits around the contact point of crossed cylinders of amorphous silica, the material of the cylindrical discs that normally support the mica sheets.

Our results demonstrate convincingly that deposition of crystals may occur from vapor without supersaturation. The requirement is a wedge-shaped cavity that allows the capillary condensation of liquid below $T_m$. The observed undercoolings of the studied substances are similar to those reported for homogeneous nucleation from the melt in water, where experimental values of the nucleation rate at $\Delta T$ = 35 K vary from $10^{11}$ to $10^{13}$ m$^{-3}$ s$^{-1}$ and from $10^{13}$ to $10^{15}$ m$^{-3}$ s$^{-1}$ $\Delta T$ = 38 K.[28] The volume $V$ of the annular capillary condensates is approximately $\pi Rh^2$;[23] therefore, V $\approx 10^{-17}$ m$^3$ for $\Delta T$ = 35–38


dx.doi.org/10.1021/jz300450g | J. Phys. Chem. Lett. XXXX, XXX, XXX–XXX

K, which would give nucleation times of the order of microseconds to milliseconds. Our results could hence be explained purely in terms of classical homogeneous nucleation of the solid in the liquid capillary condensates. However, in view of the large uncertainties involved, we cannot rule out heterogeneous nucleation of crystals on the mica surface or some enhancement of nucleation rates due to the presence of a three-phase line, as has been shown experimentally[29] and in computer simulations[30]

Although performed with model compounds, these results are highly relevant to many crystallization phenomena. The atmospheric nucleation of ice on solid aerosol particles has been proposed to occur via capillary condensation of supercooled liquid water in surface cavities,[31,32] and our results now show that this may indeed be a viable mechanism. Given that atmospheric nucleation of ice on aerosol particles is a major determinant of the earth's climate, the importance of such a route to nucleation cannot be understated. It has also been shown that nanoscale pits or pores can enhance nucleation rates of proteins[4,33,34] and small molecules,[35] particularly when the interactions between the nucleating substance and the surface are favorable. A simulation study has discussed this enhancement in terms of capillary condensation of fluid in surface pits,[36] in direct analogy with what we have now demonstrated. Because crystallization of proteins is a prerequisite for structure determination with diffraction techniques, pathways that enhance nucleation rates are of great importance to medicine and biology. Finally, a similar phenomenon in homogeneous nucleation has been suggested by recent computer simulations showing that crystal nucleation from vapor may proceed via liquid precursor droplets.[37,38]

In summary, nucleation and subsequent rapid growth of crystals will occur in liquid capillary condensates formed from saturated vapor at undercoolings equivalent to those required for bulk liquids to freeze by homogeneous nucleation. Deposition of crystals from vapor is hence possible without any supersaturation of the vapor phase given the appropriate surface topography. Although this has been the subject of theoretical discussions, we believe that our work for the first time confirms this experimentally. It would be of interest to investigate whether crystal nucleation might also be enhanced in other processes, such as the formation of crystalline biominerals like calcite and hydroxyapatite via an amorphous phase.[39] If the amorphous phase were to have a lower contact angle on the substrate than the crystal in a surface cavity, then deposition of the amorphous phase in a surface cavity could be preferable over direct crystal deposition. Recent discoveries of amorphous precursor phases in several other systems[40,41] can only serve to increase the possible importance of such a process.

## EXPERIMENTAL METHODS

A more complete description of the experimental methods is given in the Supporting Information. Muscovite mica (Paramount Corp., NY) was cleaved to 2−5 $\mu$m thickness, melt-cut into ∼1 cm$^2$ sheets, and coated with 50 nm of Ag by thermal evaporation at $p = 10^{-6}$ mm of Hg. Two mica sheets were glued with the silvered side down on silica discs ($R$ = 2 cm) with epoxy (Epikote 1004). The discs were mounted in a crossed-cylinder configuration with the lower disc on a rigid support (spring constant > $10^5$ N m$^{1-}$) inside of the stainless steel chamber of the simplified SFA[19,20] housed in a temperature-controlled enclosure.[14] The opposing, back-silvered mica surfaces formed an interferometer through which only discrete wavelengths of incident white light pass. These fringes of equal chromatic order were recorded with a CCD (charge coupled device) camera at the exit slit of a monochromator and the standard interferometry equations[42] employed to give the surface separation to ±0.2 nm.

The zero of separation (mica−mica contact) was measured in $N_2$ at $T$ = 22 °C, and a few grams of hexamethylcyclotrisiloxane (98%, ACROS), *neo*-pentanol (99% Sigma-Aldrich), or norbornane (98% Sigma-Aldrich, used as received) were then introduced to saturate the chamber atmosphere. Saturation, assumed after experimental observations were unchanged on subsequent days, took 3−4 days. In a typical experiment, the surfaces were brought together slowly with a piezoelectric positioner until they jumped together. The condensate size $h$ (Figure 1) was measured by locating a discontinuity in the fringes at the location of the liquid−vapor interface (Figure 2c−f). The behavior upon increasing and decreasing the applied force and upon separation of the surfaces was determined. After several repeat cycles, the surfaces were separated, and the temperature was changed with overnight equilibration. The reproducibility was checked by going up and down in temperature. The temperature was measured to ±0.1 °C with a Pt thermometer ∼2 cm from the surfaces.

## ASSOCIATED CONTENT

### Supporting Information

Metastability of condensed liquid in an annular wedge, extended experimental methods section, and table of physical properties of the substances used. This material is available free of charge via the Internet at http://pubs.acs.org.

## AUTHOR INFORMATION

### Corresponding Author

*E-mail: h.k.christenson@leeds.ac.uk.

### Notes

The authors declare no competing financial interest.

## ACKNOWLEDGMENTS

H.K.C. and T.K. thank the Leverhulme Trust (Grant F/10 101/B), and F.C.M. thanks the EPSRC for financial support.

## REFERENCES

(1) ten Wolde, P. R.; Frenkel, D. Enhancement of Protein Crystal Nucleation by Critical Density Fluctuations. *Science* **1997**, *277*, 1975−1978.

(2) Yau, S.-T.; Vekilov, P. G. Quasi-planar Nucleus Structure in Apoferritin Crystallisation. *Nature* **2000**, *406*, 494−497.

(3) Stradner, A.; Sedgwick, H.; Cardinaux, F.; Poon, W. C. K.; Egelhaaf, S. U.; Schurtenberger, P. Equilibrium Cluster Formation in Concentrated Protein Solutions and Colloids. *Nature* **2004**, *432*, 492−495.

(4) Sear, R. P. Nucleation: Theory and Applications to Protein Solutions and Colloidal Suspensions. *J. Phys.: Condens. Matter* **2007**, *19*, 033101.

(5) Erdemir, D.; Lee, A. Y.; Myerson, A. S. Nucleation of Crystals from Solution: Classical and Two-Step Models. *Acc. Chem. Res.* **2009**, *42*, 621−629.

(6) Savage, J. R.; Dinsmore, A. D. Experimental Evidence for Two-Step Nucleation in Colloidal Crystallisation. *Phys. Rev. Lett.* **2009**, *102*, 198302.

(7) Vekilov, P. G. Nucleation. *Cryst. Growth Des.* **2010**, *10*, 5007−5019.

(8) Garetz, B. A.; Matic, J.; Myerson, A. S. Polarization Switching of Crystal Structure in the Nonphotochemical Light-Induced Nucleation of Supersaturated Aqueous Glycine. *Phys. Rev. Lett.* **2002**, *89*, 175501.
(9) Kimura, M. Characterization of the Dense Liquid Precursor in Homogeneous Crystal Nucleation Using Solution State Nuclear Magnetic Resonance Spectroscopy. *Cryst. Growth Des.* **2006**, *6*, 854−860.
(10) Murray, B. J.; Wilson, T. W.; Dobbie, S.; Cui, Z. Q.; Al-Jumur, S.; Mohler, O.; Schnaiter, M.; Wagner, R.; Benz, S.; Niemand, M.; et al. Heterogeneous Nucleation of Ice Particles on Glassy Aerosols under Cirrus Conditions. *Nat. Geosci.* **2010**, *3*, 233−237.
(11) Turnbull, D. Kinetics of Heterogeneous Nucleation. *J. Chem. Phys.* **1950**, *18*, 198−203.
(12) Scholl, C. A.; Fletcher, N. H. Decoration Criteria for Surface Steps. *Acta Metall.* **1970**, *18*, 1083−1086.
(13) Nowak, D.; Christenson, H. K. Capillary Condensation of Water between Mica Surfaces above and below Zero-Effect of Surface Ions. *Langmuir* **2009**, *25*, 9908−9912.
(14) Nowak, D.; Heuberger, M.; Zäch, M.; Christenson, H. K. Thermodynamic and Kinetic Supercooling of Liquid in a Wedge-Pore. *J. Chem. Phys.* **2008**, *129*, 154509.
(15) Osthoff, R. C.; Grubb, W. T.; Burkhard, C. A. Physical Properties of Organosilicon Compounds I. Hexamethylcyclotrisiloxane and Octamethylcyclotetrasiloxane. *J. Am. Chem. Soc.* **1953**, *75*, 2227−2229.
(16) *Handbook of Chemistry and Physics*, 57th ed.; Weast, R. C., Ed.; CRC Press: Cleveland, OH, 1976.
(17) *Industrial Chemicals*; Faith, W. L., Keyes, D. B., Clark, R. L., Eds.; Wiley & Sons: New York, 1957; pp 109−114.
(18) Verevkin, S. P.; Emel'yanenko, V. N. The Enthalpy of Formation and Strain of Norbornane from Thermochemical Measurements and from Ab Initio Calculations. *J. Phys. Chem. A* **2004**, *108*, 6575−6580.
(19) Christenson, H. K.; Yaminsky, V. V. Adhesion and Solvation Forces between Surfaces ion Liquids Studied by Vapor-Phase Experiments. *Langmuir* **1993**, *9*, 2448−2454.
(20) Wanless, E. J.; Christenson, H. K. Interaction between Surfaces in Ethanol — Adsorption, Capillary Condensation and Solvation Forces. *J. Chem. Phys.* **1994**, *101*, 4260−4267.
(21) Christenson, H. K. Capillary Condensation Due to Van Der Waals Attraction in Wet Slits. *Phys. Rev. Lett.* **1994**, *73*, 1821.
(22) Qiao, Y.; Christenson, H. K. Triple-Point Wetting and Liquid Condensation in a Slit Pore. *Phys. Rev. Lett.* **1999**, *83*, 1371−1374.
(23) Maeda, N.; Christenson, H. K. Direct Observation of Surface Effects on the Freezing and Melting of an n-Alkane. *Colloids Surf., A* **1999**, *159*, 135−148.
(24) Christenson, H. K. Phase Behaviour in Slits — When Tight Cracks Stay Wet. *Colloids Surf., A* **1997**, *123*−*124*, 355.
(25) Christenson, H. K. Surface Deformations in Direct Force Measurements. *Langmuir* **1996**, *12*, 1404−1405.
(26) Sill, R. C.; Skapski, A. S. Method for Determining the Surface Tension of Solids, from Their Melting Points in Thin Wedges. *J. Chem. Phys.* **1957**, *24*, 644−651.
(27) Evans, R.; Marini Bettolo Marconi, U. The Role of Wetting Films in Capillary Condensation and Rise: Influence of Long-Range Forces. *Chem. Phys. Lett.* **1985**, *114*, 415−422.
(28) Murray, B. J.; Broadley, S. L.; Wilson, T. W.; Bull, S.; Wills, R. H.; Christenson, H. K.; Murray, E. J. Kinetics of the Homogeneous Freezing of Water. *Phys. Chem. Chem. Phys.* **2010**, *12*, 10380−10387.
(29) Shaw, R. A.; Durant, A. J.; Mi, Y. Heterogenous Surface Crystallisation Observed in Undercooled Water. *J. Phys. Chem. B* **2005**, *109*, 9865.
(30) Sear, R. P. Nucleation at Contact Lines Where Fluid−Fluid Interfaces Meet Solid Surfaces. *J. Phys.: Condens. Matter* **2007**, *19*, 466106.
(31) Fukuta, N. Activation of Atmospheric Particles as Ice Nuclei in Cold and Dry Air. *J. Atmos. Sci.* **1966**, *23*, 741−750.
(32) Fletcher, N. H. Active Sites and Ice Crystal Nucleation. *J. Atmos. Sci.* **1969**, *26*, 1266−1271.
(33) Chayen, N. E.; Saridakis, E.; Sear, R. P. Experiment and Theory for Heterogeneous Nucleation of Protein Crystals in a Porous Medium. *Proc. Natl. Acad. Sci. U.S.A.* **2006**, *103*, 597−601.
(34) Sugahara, M.; Asada, Y.; Morikawa, Y.; Kageyama, Y.; Kunishima, N. Nucleant-Mediated Protein Crystallization with the Application of Microporous Synthetic Zeolites. *Acta Crystallogr., Sect. D* **2008**, *64*, 686−695.
(35) Diao, Y.; Harada, T.; Myerson, A. S.; Hatton, T. A.; Trout, B. L. The Role of Nanopore Shape in Surface-Induced Crystallization. *Nat. Mater.* **2011**, *10*, 867−871.
(36) van Meel, J. A.; Sear, R. P.; Frenkel, D. Design Principles for Broad-Spectrum Protein−Crystal Nucleants with Nanoscale Pits. *Phys. Rev. Lett.* **2010**, *105*, 205501.
(37) Chen, B.; Kim, H.; Keasler, S. J.; Nellas, R. B. An Aggregation-Volume-Bias Monte Carlo Investigation on the Condensation of a Lennard-Jones Vapor below the Triple Point and Crystal Nucleation in Cluster Systems: An In-Depth Evaluation of the Classical Nucleation Theory. *J. Phys. Chem. B* **2008**, *112*, 4067−4078.
(38) van Meel, J. A.; Page, A. J.; Sear, R. P.; Frenkel, D. Two-Step Vapor-Crystal Nucleation Close below Triple Point. *J. Chem. Phys.* **2008**, *129*, 204505.
(39) Meldrum, F. C. Calcium Carbonate in Biomineralization and Biomimetic Chemistry. *Int. Mater. Rev.* **2003**, *48*, 187−224.
(40) Wolf, S. E.; Muller, L.; Barrea, R.; Kampf, C. J.; Leiterer, J.; Panne, U.; Hoffmann, T.; Emmerling, F.; Tremel, W. Carbonate-Coordinated Metal Complexes Precede the Formation of Liquid Amorphous Mineral Emulsions of Divalent Metal Carbonates. *Nanoscale* **2011**, *3*, 1158−1165.
(41) Wang, Y. W.; Kim, Y.-Y.; Christenson, H. K.; Meldrum, F. C. A New Precipitation Pathway for Calcium Sulfate Dihydrate (Gypsum) via Amorphous and Hemihydrate Intermediates. *Chem. Commun.* **2012**, *48*, 504−506.
(42) Israelachvili, J. N. Multiple-Beam Interferometry. *J. Colloid Interface Sci.* **1973**, *44*, 259.